Article

Experimental Observation of the Transition between Gas-Phase and Aqueous Solution Structures for Acetylcholine, Nicotine, and Muscarine Ions

Mahamadou Seydou, Gilles Grgoire, Jean Liquier, J. Lemaire, Jean Pierre Schermann, and Charles Desfranois

J. Am. Chem. Soc., **2008**, 130 (12), 4187-4195 • DOI: 10.1021/ja710040p

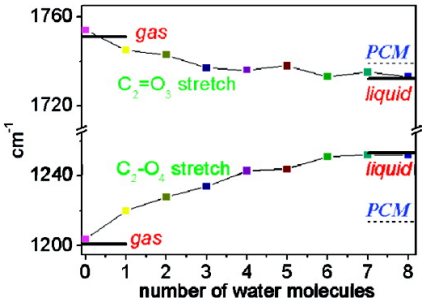

More About This Article

Additional resources and features associated with this article are available within the HTML version:

- Supporting Information
- Links to the 1 articles that cite this article, as of the time of this article download
- Access to high resolution figures
- Links to articles and content related to this article
- Copyright permission to reproduce figures and/or text from this article

View the Full Text HTML

J|A|C|S
ARTICLES
Published on Web 03/01/2008

Experimental Observation of the Transition between Gas-Phase and Aqueous Solution Structures for Acetylcholine, Nicotine, and Muscarine Ions

Mahamadou Seydou,[†] Gilles Grégoire,[†] Jean Liquier,[‡] J. Lemaire,[§] Jean Pierre Schermann,*[,†] and Charles Desfrançois[†]

Laboratoire de Physique des lasers, UMR 7538 CNRS, Université Paris 13, 93430 Villetaneuse, France, Laboratoire de Biophysique Moléculaire, Cellulaire et Tissulaire UMR 7033 CNRS, Université Paris 13, 93017 Bobigny, France, and Laboratoire de Chimie Physique, UMR 8000 CNRS, Université Paris XI, Bat. 350, 91405 Orsay Cedex, France

Received November 6, 2007; E-mail: scherman@galilee.univ-paris13.fr

Abstract: Structural information on acetylcholine and its two agonists, nicotine, and muscarine has been obtained from the interpretation of infrared spectra recorded in the gas-phase or in low pH aqueous solutions. Simulated IR spectra have been obtained using explicit water molecules or a polarization continuum model. The conformational space of the very flexible acetylcholine ions is modified by the presence of the solvent. Distances between its pharmacophoric groups cover a lower range in hydrated species than in isolated species. A clear signature of the shift of protonation site in nicotine ions is provided by the striking change of their infrared spectrum induced by hydration. On the contrary, structures of muscarine ions are only slightly influenced by the presence of water.

1. Introduction

Molecular recognition of acetylcholine and its agonists by nicotinic or muscarinic acetylcholine receptors is a widely studied topic due to its importance in memory, cognition, and reward processes as well as its potential implications in the treatment of Alzheimer's disease and Parkinson's disease.[1,2] In particular, the ligand-induced conformational changes in the receptor ligand-binding region have been studied by means of molecular dynamics simulations.[3] Acetylcholine is a key neurotransmitter in the central and peripheral nervous systems of vertebrates and insects.[4] Although plants, bacteria, or fungi do not contain any nervous system, this molecule is also found in those living bodies.[5]

In its bioactive form, the acetylcholine neurotransmitter is positively charged as well as its competitive agonists, nicotine and muscarine.[6−9] They possess either a trimethyl ammonium group or a protonated tertiary ammonium group.[10,11] Among the key elements for biorecognition of those molecules in the binding sites of the receptors, called "pharmacophores", are a cation$-\pi$ interaction between the positively charged end that interacts preferentially with aromatic aminoacids[12−14] and an accepting hydrogen bond interaction with receptor residues.[15] The distance between these two pharmacophoric sites is thus a crucial parameter that is usually invoked for explaining the strong biochemical similarities observed between acetylcholine and either nicotine or muscarine.[7,16−18] Those molecules possess several close-lying conformers, and the distance between their recognition sites can vary strongly from one conformer to another. They have been the subject of several theoretical studies concerning the determination of their different conformers in vacuum,[16,18,19] in solution,[16,18,20−23] or in crystals.[24] However, those predictions have not already been directly confronted with

[†] Laboratoire de Physique des lasers, Université Paris 13.
[‡] Laboratoire de Biophysique Moléculaire, Université Paris 13.
[§] Université Paris XI.

(1) Domino, E. F. *Neuropsychopharmacology* **1998**, *18*, 456.
(2) Hammond, P. S.; Wu, Y.; Harris, R.; Minehardt, T. J.; Car, R.; Schmitt, J. D. *J. Comput.-Aided. Mol. Des.* **2005**, *19*, 1.
(3) Henchman, R. H.; Wang, H. L.; Sine, S. M.; Taylor, P.; McCammon, J. A. *Biophys. J.* **2005**, *88*, 2564.
(4) Yuan, H.; Petukhov, P. A. *Bioorg. Med. Chem.* **2006**, *14*, 7936.
(5) Kawashima, K.; Misawa, H.; Moriwaki, Y.; Fujii, Y. X.; Fujii, T.; Horiuchi, Y.; Yamada, T.; Imanaka, T.; Kamekura, M. *Life Sci.* **2007**, *80*, 2206.
(6) Graton, J.; Berthelot, M.; Gal, J. F.; Girard, S.; Laurence, C.; Lebreton, J.; Le Questel, J. Y.; Maria, P. C.; Naus, P. *J. Am. Chem. Soc.* **2002**, *124*, 10552.
(7) Cashin, A. L.; Petersson, E. J.; Lester, H. A.; Dougherty, D. A. *J. Am. Chem. Soc.* **2005**, *127*, 350.
(8) Woods, A. S. *J. Proteome Res.* **2004**, *3*, 478.
(9) Lee, W. Y.; Sine, S. M. *Nature* **2005**, *438*, 243.
(10) Karlin, A. *Pharmacogenomics J.* **2001**, *1*, 221.
(11) Arnaud, V.; Berthelot, M.; Evain, M.; Graton, J.; Le Questel, J. Y. *Chem.—Eur. J.* **2007**, *13*, 1499.
(12) Zhong, W. G.; Gallivan, J. P.; Zhang, Y. O.; Li, L. T.; Lester, H. A.; Dougherty, D. A. *Proc. Natl. Acad. Sci. U.S.A.* **1998**, *95*, 12088.
(13) Schmitt, J. D.; Sharples, G. V.; Caldwell, W. S. *Med. Chem.* **1999**, *42*, 3066.
(14) Beene, D. L.; Brandt, G. S.; Zhong, W. G.; Zacharias, N. M.; Lester, H. A.; Dougherty, D. A. *Biochemistry* **2002**, *41*, 10262.
(15) Biot, C.; Buisine, E.; Kwasigroch, J. M.; Wintjens, R.; Rooman, M. *J. Biol. Chem.* **2002**, *277*, 40816.
(16) Elmore, D. E.; Dougherty, D. A. *J. Org. Chem.* **2000**, *65*, 742.
(17) Graton, J.; van Mourik, T.; Price, S. L. *J. Am. Chem. Soc.* **2003**, *125*, 5988.
(18) Munoz-Caro, C.; Nino, A.; Mora, M.; Reyes, S.; Melendez, F. J.; Castro, M. E. *THEOCHEM* **2005**, *726*, 115.
(19) Segall, M. D.; Payne, M. C.; Boyes, R. N. *Mol. Phys.* **1998**, *93*, 365.
(20) Vistoli, G.; Pedretti, A.; Testa, B.; Matucci, R. *Arch. Biochem. Biophys.* **2007**, *464*, 112.
(21) Vistoli, G.; Pedretti, A.; Villa, L.; Testa, B. *J. Am. Chem. Soc.* **2002**, *124*, 7472.
(22) Vistoli, G.; Pedretti, A.; Villa, L.; Testa, B. *J. Med. Chem.* **2005**, *48*, 6926.
(23) Marino, T.; Russo, N.; Tocci, E.; Toscano, M. *Theor. Chem. Acc.* **2001**, *107*, 8.
(24) Chothia, C.; Pauling, P. *Proc. Natl. Acad. Sci. U.S.A.* **1970**, *65*, 477.

10.1021/ja710040p CCC: $40.75

experimental results. Gas-phase studies are often conducted by means of either microwave spectroscopy,[25] which does not apply to charged systems, or infrared/resonant two-photon ionization spectroscopy (IR/R2PI), which usually[26] but not necessarily[27] requires the presence of a UV chromophore.

In the present work, we present the first gas-phase experimental spectroscopic studies of acetylcholine, nicotine, and muscarine ions in the infrared range. We compare these results to those obtained in aqueous solution. We wish to examine if well-defined conformers, clearly identified as calculated lowest-energy structures and possibly observable in experiments conducted at low temperatures,[27,28] do persist or, on the contrary, are washed out in experiments conducted at a physiologically relevant temperature of 300 K either in the gas phase or in aqueous solution. Another goal is to investigate if distances between pharmacophoric groups can be experimentally monitored in mass-selected species.

After describing the experimental methods and the computational approaches used for interpretation, we will first consider structures of acetylcholine, muscarine, and nicotine ions isolated in the gas phase. We will then investigate how the presence of water influences conformer structures and protonation sites. The relationship between those structures and bioactivity determined in pharmaceutical studies will then be examined.

2. Experimental and Computational Methods

In the case of gas-phase ions, direct observation of infrared radiation absorption is unfortunately hindered by the extremely low available ionic densities. However, Infrared MultiPhoton Dissociation (IRMPD) offers a precious alternative.[29−34] A detailed analysis of the IRMPD process can be found in ref 35. Infrared spectroscopy in the fingerprint spectral region (800−2000 cm^{-1}) becomes accessible for the determination of gas-phase biomolecular structures.[34,36−38] The experimental procedure used in the present work has been described previously.[39] In brief, ions produced by electrospray from solutions are confined in a Bruker Esquire 3000 quadrupole ion trap mass spectrometer[40] and illuminated by the high-power and high-repetition rate infrared beam issued from the free-electron laser CLIO.[41] Mass-selected ions absorb photons that bring them from a $v_i = 0$ to a $v_f = 1$ vibrational state. Between two photon absorptions, internal vibrational redistribution (IVR) takes place and brings back ions to their initial $v_i = 0$ vibrational state while the acquired internal energy is redistributed over other modes. Following absorption of many photons, dissociation takes place. Infrared absorption is then monitored through detection of the ionic fragmentation yield. It is worthwhile to note that, in IRMPD experiments, fragmentation yields involve highly excited vibrational states and thus depend upon IVR rates. Experimental intensities in the spectral dependence of the fragmentation yields do not necessarily correspond to the predicted intensities. Only positions of spectral lines in IRMPD spectra reflect the infrared absorption spectrum (with some possible small red-shifts[35]). Intensities of localized vibrational modes weakly coupled to delocalized modes involved in fragmentation can be strongly reduced.

In order to experimentally compare isolated gas-phase ion structures to their counterpart in water, an ideal situation would be to record the infrared absorption spectra of mass-selected clusters obtained by adding water molecules sequentially,[42] until a full hydration layer is reached. Unfortunately, this systematic method has only been applied, up to now, to cold ionic molecular clusters containing chromophores and a very restricted number of water molecules.[28] The here employed use of IRMPD in a quadrupole trap in the presence of a buffer gas precludes the production of clusters. We thus choose to record infrared spectra of acetylcholine, nicotine, and muscarine solutions. In order to record IR spectra of positively charged ions, acetylcholine, nicotine, and muscarine solutions were acidified (pH = 2) by adding 5 μL of aqueous solutions of acetylcholine, nicotine, and muscarine and 5 μL of 0.1 M HCl solution. After homogenization, 2 μL of the acidified solutions were deposited on a KBr slide and the IR spectra were recorded with a FT-IR Brucker Tensor 27 (2 cm^{-1} resolution). Due to the absorption of water, the spectra were only recorded in the 800−1700 cm^{-1} fingerprint region similar to that of the CLIO FEL laser.

Interpretation of gas-phase experimental infrared spectra has been conducted by means of structure calculations and vibrational analysis. A first systematic search of the lowest-energy structures has been performed with both the Amber force-field and the semiempirical AM1 method. Each structure has then been optimized at the B3LYP/6-31G*, B3PW91/6-311++G**, and MP2/6-31G* levels. Since the gas-phase experiments have been conducted at 300 K, molecular dynamics simulations have been performed in order to evaluate the possibility of interconversion between the different conformations identified as minima of the potential energy landscape. Those simulations conducted at the HF/6-31G* level were run at a temperature of 500 K rather than 300 K in order to accelerate the exploration. In the first step, the corresponding infrared absorption spectra, covering the whole experimental spectral range from 800 to 2000 cm^{-1} ("broad-band" spectra), have been simulated from calculated frequencies ν_{cal} using either the B3LYP/6-31G* level with the recommended uniform scaling factor of 0.9614 or the B3PW91/6-311++G** level with the linearly dependent scaling factor $\nu_{exp} = 0.955\ \nu_{cal} + 25.7$ (in cm^{-1}).[43] Each line is convoluted by a Lorentzian (15 cm^{-1} fwhm). Both levels provide fair agreements between predicted and experimentally recorded spectra in between 1000 and 2000 cm^{-1}, but only the latter is acceptable in between 800 and 1000 cm^{-1}. Those "broad-band" spectra can allow relatively clear distinctions between different configurations, for example in the case of different protonation sites leading to the appearance or disappearance of characteristic spectral lines.

The problem becomes more subtle in the case of relatively close conformations leading to only small spectral shifts. In conformer-selective IR-R2PI experiments conducted on very-low-temperature

(25) Cocinero, E. J.; Lesarri, A.; Sanz, M. E.; Lopez, J. C.; Alonso, J. L. *ChemPhysChem* **2006**, *7*, 1481.
(26) Macleod, N. A.; Simons, J. P. *Phys. Chem. Chem. Phys.* **2004**, *6*, 2821.
(27) Vaden, T. D.; de Boer, T. S. J. A.; Macleod, N. A.; Marzluff, E. M.; Simons, J. P.; Snoek, L. C. *Phys. Chem. Chem. Phys* **2007**, *9*, 2549.
(28) Kamariotis, A.; Boyarkin, O. V.; Mercier, S. R.; Beck, R. D.; Bush, M. F.; Williams, E. R.; Rizzo, T. R. *J. Am. Chem. Soc.* **2006**, *128*, 905.
(29) Asmis, K. R.; Brümmer, M.; Kaposta, C.; Sambrogio, G.; von Helden, G.; Meijer, G.; Rademann, K.; Wöste, L. *Phys. Chem. Chem. Phys.* **2002**, *4*, 1101.
(30) Oh, H. B.; Lin, C.; Hwang, H. Y.; Zhai, H. L.; Breuker, K.; Zabrouskov, V.; Carpenter, B. K.; McLafferty, F. W. *J. Am. Chem. Soc.* **2005**, *127*, 4076.
(31) Polfer, N. C.; Oomens, J.; Dunbar, R. C. *Phys. Chem. Chem. Phys*. **2006**, *8*, 2744.
(32) Breuker, K. *Int. J. Mass Spectrom.* **2004**, *239*, 33.
(33) Lucas, B.; Gregoire, G.; Lemaire, J.; Maitre, P.; Glotin, F.; Schermann, J. P.; Desfrancois, C. *Int. J. Mass Spectrom.* **2005**, *243*, 105.
(34) Kapota, C.; Lemaire, J.; Maitre, P.; Ohanessian, G. *J. Am. Chem. Soc.* **2004**, *126*, 1836.
(35) Oomens, J.; Sartakov, B. G.; Meijer, G.; von Helden, G. *Int. J. Mass Spectrom.* **2006**, *254*, 1.
(36) Carcabal, P.; Kroemer, R. T.; Snoek, L. C.; Simons, J. P.; Bakker, J. M.; Compagnon, I.; Meijer, G.; von Helden, G. *Phys. Chem. Chem. Phys.* **2004**, *6*, 4546.
(37) Polfer, N. C.; Paizs, B.; Snoek, L. C.; Compagnon, I.; Suhai, S.; Meijer, G.; von Helden, G.; Oomens, J. *J. Am. Chem. Soc.* **2005**, *127*, 8571.
(38) Polfer, N. C.; Valle, J. J.; Moore, D. T.; Oomens, J.; Eyler, J. R.; Bendiak, B. *Anal. Chem.* **2006**, *78*, 670.
(39) Gregoire, G.; Gaigeot, M. P.; Marinica, D. C.; Lemaire, J.; Schermann, J. P.; Desfrançois, C. *Phys. Chem. Chem. Phys.* **2007**, *9*, 3082.
(40) Mac Aleese, L.; Simon, A.; McMahon, T. B.; Ortega, J. M.; Scuderi, D.; Lemaire, J.; Maitre, P. *Int. J. Mass Spectrom.* **2006**, *249*, 14.
(41) Lemaire, J.; Boissel, P.; Heninger, M.; Mauclaire, G.; Bellec, G.; Mestdagh, H.; Simon, A.; Caer, S. L.; Ortega, J. M.; Glotin, F., et al. *Phys. Rev. Lett* **2002**, *89*, 273002.
(42) Blom, M. N.; Compagnon, I.; Polfer, N.; von Helden, G.; Meijer, G.; Suhai, S.; Paizs, B.; Oomens, J. *J. Phys. Chem.* **2007**, *111*, 7309.
(43) Gornicka, E.; Rode, J. E.; Raczynska, E. D.; Dasiewicz, B.; Dobrowolski, J. C. *Vib. Spectrosc.* **2004**, *36*, 105.

species,[28,44−47] it is possible to obtain assignments of the isomer-selected experimental spectra by comparison to predicted IR spectra corresponding to the different conformers. In the present work, the situation is different since the experiment is conducted at 300 K. For a given ionic species, different populated conformations are simultaneously observed and the experimental IRMPD spectrum is thus a weighted sum of the different corresponding spectral contributions. In order to establish a correspondence between conformations and some specific spectral lines, we here employ "local" or "narrow-band" scaling factors that are determined by least-square adjustments between experimental and predicted values of specific structure-sensitive spectral lines. The only constraint concerning these local scaling factors is that they must be identical for a given vibration (e.g., a C−O stretch) existing in a given molecule or in different molecules. We then admit that the anharmonicity of a given vibrational mode remains the same in the different conformations although it varies from one vibrational mode to another.

The conformational distributions of acetylcholine, nicotine, and muscarine in aqueous solution have already been theoretically investigated by means of the Polarization Continuum Model. (PCM).[18] Since we are interested in the comparison between gas-phase and solution infrared spectra, we here use both cluster structure calculations with explicit water molecules[48−51] and a PCM model. Vibrational spectra of clusters containing a number of water molecules varying from one to eight have thus been calculated at the B3LYP/6-31G* level with the recommended uniform scaling factor of 0.9614. The initial geometries of those clusters have been chosen in an attempt to take into account the situation encountered by water molecules in solution. Some water molecules are directly bound to the hydrophilic sites of the considered molecules. They correspond to the first solvation layer (interstitial water) and are those generally considered in hydrated cluster studies. In solution, they are also bound to bulk water molecules of higher-rank layers. For computations, we try to limit as much as possible the number of water molecules in our attempt to reproduce as best as possible the recorded spectra. We restrict the initial cluster conformations to "droplets" into which water molecules are bound both to the infrared "chromophores" of the considered molecules, C═O or N−H groups for example, and between themselves in cyclic structures. This allows us to simulate the influence of several hydration layers.

Each calculated spectral line is then convoluted by a Lorentzian (5 cm^{-1} fwhm). Those condensed-phase spectral line shapes are narrower than the corresponding gas-phase line shapes. In FT-IR, we measure the true IR absorption spectra while the IRMPD spectra are broadened by absorption of hot bands due to the multiphoton absorption process[35] and excitation of low-frequency sequence bands. More sophisticated methods such as torsional analysis[52] and quantum dynamics simulations (CPMD)[2] would most probably be more appropriate for determination of structures and interpretation of infrared spectra at 300 K.[53] However, the size of the here studied molecules would impose considerably too large amounts of computer time, and these methods are out of the scope of the present experimental work.

3. Gas-Phase Ionic Structures

In the following, we will adopt the atom numbering and the conformer nomenclature of ref 18 for the three considered molecules displayed in Figure 1. In this work, the gas-phase conformers have been labeled in increasing order of calculated energy. Each of these conformers corresponds to a minimum of the potential energy as a function of relevant torsional angles defining the geometry.

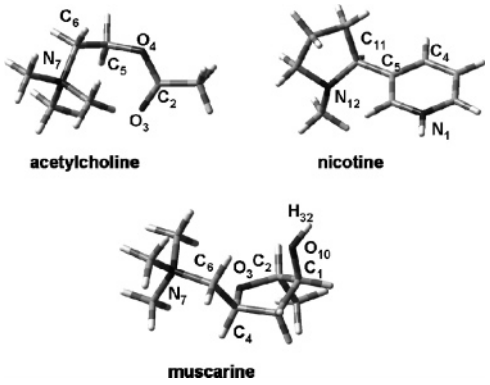

Figure 1. Structure of acetylcholine, nicotine (protonated on the pyridine cycle) and muscarine. The adopted atom numbering convention is identical to that of ref 18.

Table 1. Dihedral Angles (deg) and Energetic (kJ/mol) (ΔE and ΔG_{300K}) of the Five Lowest Energy Conformations of Gas Phase Acetylcholine Ions Calculated at the B3PW91/6-311++G** Level[a]

	I	II	III	IV	V
θ_1	280	292	294	180	203
θ_2	110	279	194	180	80
ΔE_{MP2}	0	2.12	5.82	19.39	7.79
ΔE^b	0	1.55	2.42	9.11	4.20
ΔG_{300K}	2.96	0.70	0	3.61	2.48

[a] ΔE_{MP2} values are calculated at the MP2/6-31* level. [b] Corrected by the ZPE

3.1. Acetylcholine. Acetylcholine is a flexible molecule characterized by a quaternary ammonium group (N_7) linked by a $N_7-C_6-C_5-O_4$ backbone to an acetoxy group (Figure 1). Several of its minimum energy conformers have already been identified, and the corresponding structures have been calculated at different levels of theory.[18,24] However, to our knowledge, no direct comparison to gas-phase data has already been performed. The acetoxy group is planar,[24] and the problem of conformers is thus reduced to the determination of the $N_7C_6C_5O_4$ (θ_1) and $C_6C_5O_4C_2$ (θ_2) torsion angles. Four conformers denoted from I to IV were identified in ref 18. We conducted a systematic exploration of the conformational landscape with both the Amber force field[54] and the AM1 method. The selected degrees of freedom were then the θ_1, θ_2 torsion angles with 5° systematic search steps. This exploration provided us four possible minima of the potential energy surface. Three of them, here denoted I, II, and IV, were identical to those of ref 18. In contrast, the fourth one, further denoted as conformer V with nearly the same θ_2 value as conformer I but a very different θ_1 value, was not identified in this reference. Its existence as a minimum is confirmed at the DFT and MP2 level (Supporting Information). This conformer lies 7.65 kJ/mol higher than conformer I at the MP2/cc-pVDZ level used in ref 18. The enthalpy and free energy of the five conformations along with their dihedral angles θ_1 and θ_2 calculated at the DFT/B3PW91/6-31++G** level are reported in Table 1.

(44) Brutschy, B. *Chem. Rev.* **2000**, *100*, 3891.
(45) Robertson, E. G.; Simons, J. P. *Phys. Chem. Chem. Phys.* **2001**, *3*, 1.
(46) Zwier, T. S. *J. Phys. Chem. A* **2006**, *110*, 4133.
(47) Mons, M.; Piuzzi, F.; Dimicoli, I.; Gorb, L.; Leszczynski, J. *J. Phys. Chem.* **2006**, *110*, 10921.
(48) Gaigeot, M. P.; Kadri, C.; Ghomi, M. *J. Mol. Struct.* **2001**, *565*, 469.
(49) van Mourik, T. *Phys. Chem. Chem. Phys.* **2004**, *6*, 2827.
(50) Macleod, N. A.; Johannessen, C.; Hecht, L.; Barron, L. D.; Simons, J. P. *Int. J. Mass Spectrom.* **2006**, *253*, 193.
(51) Derbel, N.; Hernandez, B.; Pflüger, F.; Liquier, J.; Geinguenaud, F.; Jaïdane, N.; Ben Lakhdar, Z.; Ghomi, M. *J. Phys. Chem. B* **2007**, *111*, 1470
(52) Miller, T. F.; Clary, D. C. *J. Phys. Chem. A* **2006**, *110*, 731.
(53) Marinica, D. C.; Gregoire, G.; Desfrancois, C.; Schermann, J. P.; Borgis, D.; Gaigeot, M. P. *J. Phys. Chem. A* **2006**, *110*, 8802.
(54) Ponder, J. W.; Case, D. A. *Adv. Protein Chem.* **2005**, *66*, 27.

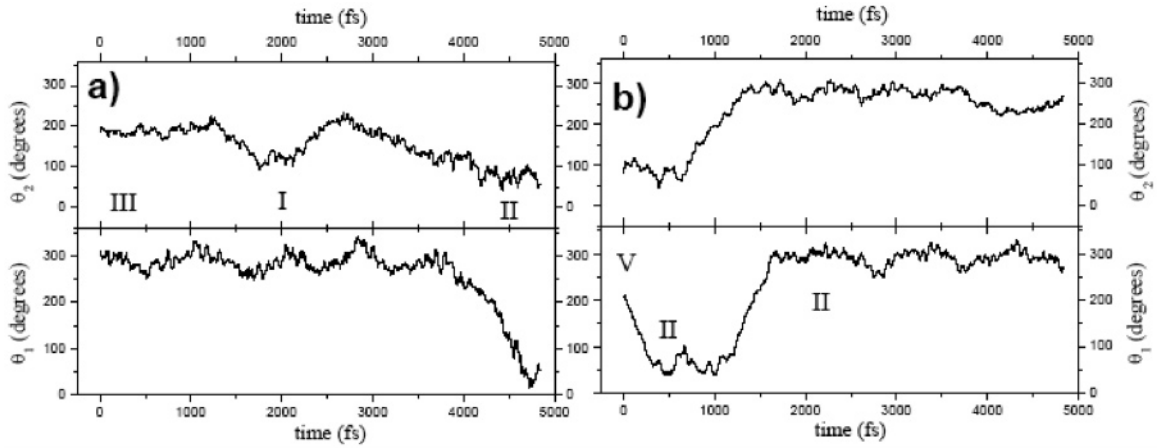

Figure 2. Time evolution of the dihedral angles θ_1 et θ_2 for HF(6-31G*)/MD simulations of acetylcholine ions conducted at 500 K starting from conformation III (a) and conformation V (b) for 5 ps.

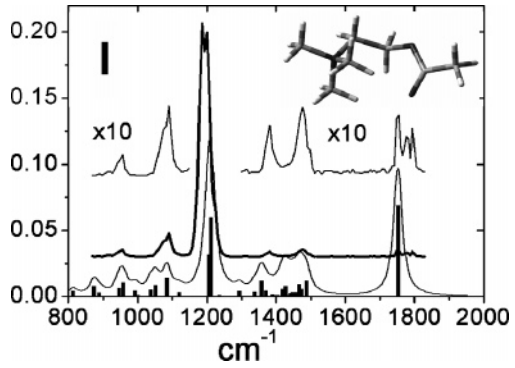

Figure 3. Comparison between the simulated IR spectrum of the gas-phase acetylcholine conformer I and the "broad-band" IRMPD experimental spectrum. The structure is calculated at the B3PW91/6-311++G** level, and vibrational frequencies are obtained with the linearly dependent scaling factor $\nu_{exp} = 0.955\nu_{cal} + 25.7$ (in cm^{-1}).

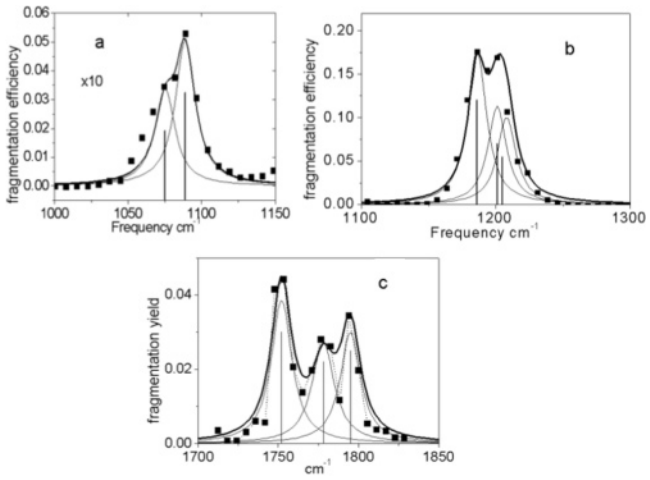

Figure 4. Experimental IRMPD spectrum in the 1000−1120 cm^{-1} range fitted by two Lorentzian lineshapes centered at 1075 and 1089 cm^{-1} (a); in the 1150−1250 cm^{-1} range fitted by free Lorentzian line shapes centered at 1186, 1200, and 1205 cm^{-1} (b); and in the 1730−1800 cm^{-1} range fitted by three Lorentzian lineshapes centered at 1751, 1778, and 1794 cm^{-1} (c).

The energy and free energy differences between the different conformers are strongly dependent upon the used level of calculation as well as the ordering between those conformers and are provided as Supporting Information. Except for conformer IV lying 9.11 kJ/mol above the most stable conformer I, energy differences between other conformers remain relatively small and similar to *kT* at the experimental temperature 300 K. Large barriers are found between some conformers, for example up to 31.7 kJ/mol between conformers II and IV. A molecular dynamics simulation conducted at a temperature of 500 K at the HF/6-31G* level shows that an acetylcholine ion initially in conformation III also explores within a few picoseconds conformations I and II but not conformations IV and V. The ion then still remains during sufficient amounts of time in each conformation to provide vibrational spectra with rather narrow spectral lines. In contrast, an acetylcholine ion initially in conformation V does not remain in this conformation and rapidly moves to conformation II (Figure 2). Based on the energetics and on the molecular dynamics simulations, we are thus lead to suppose that mainly conformers I, II, and III are experimentally populated.

The spectral dependence of the IRMPD fragmentation yield of positively charged acetylcholine ions between 800 and 1800 cm^{-1} is presented in Figure 3. The major contribution in the "broad-band" IRMPD spectrum of acetylcholine is the peak around 1200 cm^{-1}. It corresponds to the C_2-O_4 stretch. Full assignments in terms of potential energy distributions[51] of observed vibrational features are provided as Supporting Information. Among other observed weak spectral features, we only consider those corresponding to vibrations sensitive to structural changes of the backbone. The weak spectral structures around 1080 and 1770 cm^{-1}, respectively, correspond to the C_5-O_4 and $C_2=O_3$ stretches as a major contribution. They can be fitted, respectively, by two (1075 and 1089 cm^{-1}) and three (1751, 1778, and 1794 cm^{-1}) Lorentzian line shapes. The calculated intensities of the three $C_2=O_3$ stretch lines in conformers I, II, and III are nearly identical. Since the three peaks of Figure 4c have comparable amplitudes, we conclude that conformers I, II, and III are, within experimental accuracy, nearly equally populated in agreement with the molecular dynamics simulations. The major peak around 1200 cm^{-1} can be fitted by three Lorentzian line shapes. For the fit, we admit that conformers I, II, and III are populated and use the intensities of their C_2-O_4 stretches calculated at the B3PW91/6-311++G** level. The Lorentzian lineshapes are then, respectively, centered at 1186, 1201, and 1205 cm^{-1}.

Instead of using a unique scaling factor, as in the simulation of the "broad-band" spectrum, we use adjusted "local" scaling factors, respectively equal to 0.9842 for the C_2-O_4 and the C_5-

Table 2. Attribution of Experimental Frequencies to Conformations of Acetylcholine and Corresponding Frequencies Calculated at the B3PW91 Level with "Local" Scaling Factors

conformation	experimental frequencies			calculated frequencies		
I	1075	1205	1751	1082	1213	1752
II	1075	1201	1778	1077	1197	1778
III	1089	1186	1794	1089	1192	1800
IV				1067	1204	1790
V				1068	1216	1760

O_4 stretches and 0.9691 for the $C_2{=}O_3$ stretch following harmonic frequency calculations at the B3PW91/6-311++G** level. We obtain the attribution of observed spectral lines to calculated structures given in Table 2.

3.2. Nicotine. Nicotine possesses a pyridine cycle and a pyrrolidine cycle linked by a $C_5{-}C_{11}$ bond. The orientation of the methyl group of the pyrrolidine cycle with respect to the pyridine cycle defines the *cis* and *trans* conformations. Previous calculations have shown that the *cis* conformation is sterically unfavorable[16] and lies 9 kJ/mol above the *trans* conformation.[18] This *cis* conformation is not experimentally populated and will thus be ignored here. The dihedral angle ψ between the two cycles ($N_{12}{-}C_{11}{-}C_5{-}C_4$) then remains as a unique structural parameter. In protonated nicotine, two protonation sites are available, respectively, on the N_1 (sp^2) and N_{12} (sp^3) atoms of the pyridine and pyrrolidine groups. For each of these sites, in agreement with ref 18, our calculations confirm the existence of four conformations. At the MP2/6-31G* level, conformation II lies 6 kJ/mol above the lowest-energy conformation I. Conformations III and IV lie more than 10 kJ/mol above I and will thus not be considered in the interpretation of our experimental data.

Calculations at the B3PW91/6-311++G** level show that this angle is, respectively, equal to 288° and 115° for conformations I and II of nicotine protonated on the pyrrolidine site. It is equal to 165° and 323°, respectively, for conformations I and II in the case of protonation on the pyridine site, in very good agreement with calculations from refs 6 and 18, respectively obtained at the B3LYP/6-31++G** and MP2/cc-pVDZ levels. The IRMPD experimental "broad-band" spectrum of protonated nicotine is displayed in Figure 5. It exhibits three prominent peaks corresponding to N−H bends and, respectively, located at 1368, 1456, and 1539 cm^{-1}.

The striking difference between the experimental IRMPD spectrum and the predicted spectra is the absence of the prominent spectral feature at 1539 cm^{-1} in the simulated spectra corresponding to the pyrrolidine cycle protonation site. This line, corresponding to the $N_1{-}H$ bend, is present in both predicted spectra of conformations I and II of the protonated pyridine cycle. Among the four possible conformations of nicotine protonated on the pyridine cycle, the three observed main lines are only present in the predicted spectrum of the lowest-energy one (I). In particular, the observed line at 1328 cm^{-1} is missing in the predicted spectrum of conformation II. Conformation I is thus the only one experimentally populated in agreement with the energetic predictions.

The gas-phase protonation site of nicotine has already been the subject of several theoretical investigations.[16,55,56] Calculations predict the pyridine cycle as the most energetically favored site in the gas phase. The gas-phase basicities of nicotine, nornicotine (in nornicotine, the methyl group of the pyrrolidine cycle of nicotine is replaced by a hydrogen atom), and model substituted pyrrolidines have been measured in an FT-ICR spectrometer.[6] The interpretation of the experimental results by means of DFT calculations of those gas-phase basicities allowed a definitive answer in the case of nornicotine of which protonation site is the pyridine cycle. In contrast, the error bars of the calculations were such that no definitive conclusion could be drawn for nicotine and both protonation sites were assumed to be possible in the gas phase. The present study constitutes the first unequivocal experimental determination of the protonation site of nicotine in the gas phase. It confirms the theoretical predictions of its location on the pyridine cycle.[6]

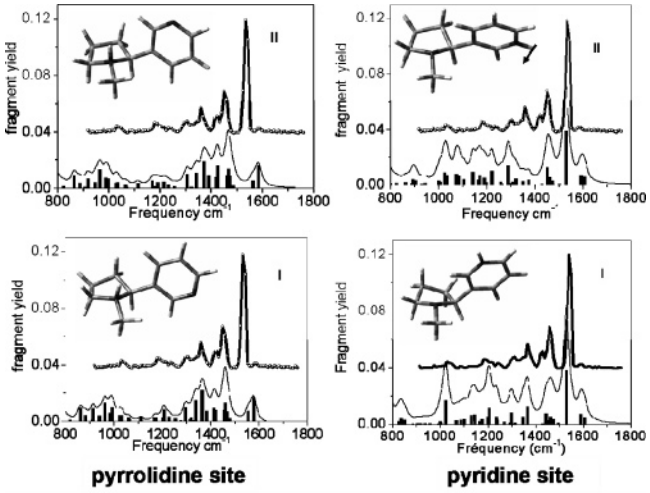

Figure 5. Comparison between the experimental IRMPD spectrum of protonated nicotine and simulated spectra corresponding to the two lowest-energy conformations I (bottom) and II (top) protonated on the pyrrolidine (left) and pyridine (right) sites.

3.3. Muscarine. The potential energy landscape of muscarine has been characterized by the $N_7C_6C_4O_3$ dihedral angle, and four "gas-phase" conformations labeled I to IV were identified in ref 18. Our systematic conformational search with both the Amber force-field and AM1 method using the $N_7C_6C_4O_3$ and $C_2C_1O_{10}H_{32}$ torsion angles as degrees of freedom with 5° search steps as well as our calculations conducted at the B3LYP/6-31++G**, MP2/6-31G**, and B3PW91/6-311++G** levels confirm the existence of these four conformations, respectively corresponding to the $N_7C_6C_4O_3$ torsion angle values equal to 55°, 325°, 288°, and 150°. In addition to these conformations, we identified two other conformations, further labeled IA and IB, possessing, within 2°, nearly the same torsion angle as that of conformation I but with different orientations of the $O_{10}H_{32}$ group. The calculated values at the B3PW/6-311++G** of the torsion angle $C_2C_1O_{10}H_{32}$ of conformations I, IA, and IB are respectively equal to 280°, 208°, and 58°. The free energy differences between conformers IA and IB with respect to conformer I are respectively equal to 1.37 and 16.5 kJ/mol. Among the six possible conformations, only the lowest-energy conformations I and IA are expected to be experimentally populated at 300 K. The comparison between the experimentally

(55) Raczynska, E. D.; Makowski, M.; Gornicka, E.; Darowska, M. *Int. J. Mol. Sci.* **2005**, *6*, 143.

(56) Koné, M.; Illien, B.; Laurence, C.; Gal, J. F.; Maria, P. C. *J. Phys. Org. Chem.* **2006**, *19*, 104.

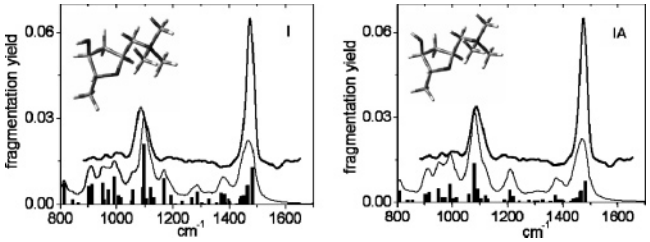

Figure 6. Comparison between the experimental "broad-band" IRMPD spectrum of muscarine ions and simulated spectra corresponding to the two lowest-energy conformations I (left) and IA (right). Those conformations differ from the $O_{10}H_{32}$ group orientation in the upper left of the structures.

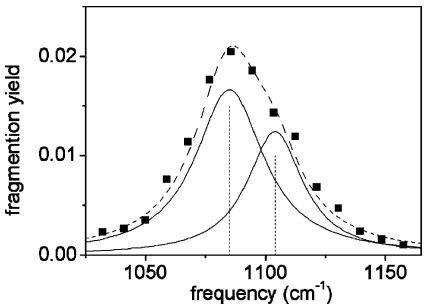

Figure 7. Experimental IRMPD spectrum of muscarine ions in the 1020−1170 cm^{-1} range fitted by two Lorentzian lineshapes centered at 1085 and 1104 cm^{-1}.

recorded and predicted broad-band IR spectra of muscarine ions is displayed in Figure 6.

Two prominent peaks are observed around 1100 and 1473 cm^{-1}. The first one is broad and corresponds to the C_2-O_3 stretch that is sensitive to the ion structure. As shown by the fit presented in Figure 7, it is the sum of the contributions of two Lorentzian lines respectively centered on 1085 and 1104 cm^{-1}. Structure optimizations and vibrational frequency calculations were conducted at the B3PW91/6-311++G** level, using the same "local" scaling factor for C−O stretches (0.9842) as in the case of acetylcholine. We obtain respective theoretical values of 1085 and 1103 cm^{-1} for the C_2-O_3 stretch of conformation I and IA. The very weak spectral line in the vicinity of 1200 cm^{-1} corresponds to the $C_1O_{10}H_{32}$ bend (a full analysis is provided as Supporting Information). It is the sum of the contributions of structure I (1205 cm^{-1}) and IA (1185 cm^{-1}). The second prominent peak around 1473 cm^{-1} is narrower and corresponds to methyl torsions that are almost insensitive to the structure.

4. Ionic Species in Aqueous Solution

Under biological conditions, the three considered molecules are not isolated but in the presence of surrounding water molecules. They possess chemical groups (e.g., CO or NH) able to establish hydrogen bonds and rather hydrophobic methyl groups. Solvation effects must be taken into account for modeling real conditions encountered in acetylcholine receptors.[57] In the present studies, the real biological conditions are clearly not met, but it is hoped that experimental studies of fully hydrated ions can give insights into the influence of hydration upon structures. At 300 K, there is no definite structure of the water environment but rather a very large set of hydrogen bonds that are continuously formed and broken.[58] We will thus here restrict the discussion to a qualitative interpretation of the observed IR spectra. Interpretation of the experimental IR spectra of ionic species in solution can be conducted by means of different methods. The water environment can be treated as a continuum. It can also be considered explicitly by adding water molecules at strategic sites in "frozen" structures[51] or more realistically in quantum dynamics calculations conducted at a finite temperature.[59] We here simply interpret our experimental spectra through comparison with simulated spectra calculated from a set of hydrated cluster structures ("explicit water").[60,61]

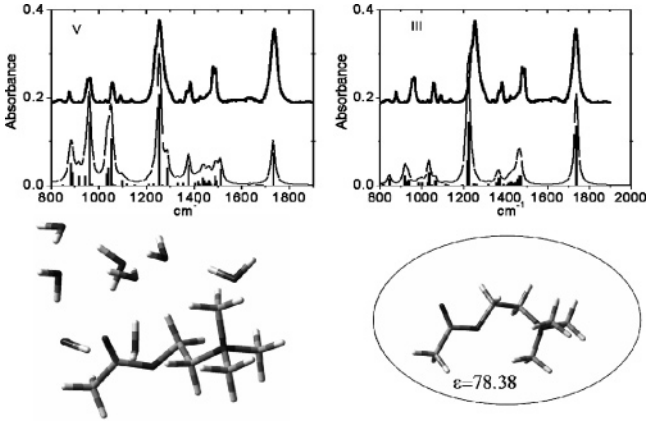

Figure 8. Experimental FT-IR and simulated absorption spectrum of acetylcholine in an acidified (pH = 2) solution in the 800−2000 cm^{-1} region. The upper left simulated spectrum corresponds to the absorption spectrum of acetylcholine in conformation V in the presence of eight water molecules (bottom left). The upper right simulated spectrum has been obtained from configuration III by means of a PCM calculation.

4.1. Acetylcholine. The broad band IR spectrum of acetylcholine in an acidified aqueous solution is displayed in Figure 8. The water absorption background has been removed by subtraction of the experimental acidified pure water spectrum. In order to evaluate the structure of its first hydration shell, we have embedded an acetylcholine ion in a cage of 146 water molecules and optimized the structure at the HF/STO-3G level. The obtained hydration shell displayed in the Supporting Information includes 40 water molecules, and full quantum calculations would be very costly. Typical distances between water molecules and the O_3 (carbonyl), O_4 (ester), and N_7 atoms are respectively equal to 2.65, 3.44, and 5.5 Å. We here restrict the calculations to water molecules that preferentially interact with the most hydrophilic group and between themselves, creating a rather rigid water droplet in the vicinity of the C═O group and submitted to charge-dipole interactions with the (N^+-$(CH_3)_3$) group.

As in the case of isolated species, a molecular dynamics simulation of acetylcholine in a dielectric continuum ($\epsilon = 78.38$) has been performed at 500 K at the HF/6-31G* level starting from configuration III and V. While in the former case, the acetylcholine ion explores the conformation II and goes back to its initial conformation III, acetylcholine in conformation V remains in its basin for the all dynamics (see Supporting Information). Unlike the isolated species, such a conformation seems to be stable and has therefore been included in the theoretical treatment of acetylcholine in solution.

(57) Zhang, D. Q.; Gullingsrud, J.; McCammon, J. A. *J. Am. Chem. Soc.* **2006**, *128*, 3019.
(58) Otting, G.; Liepinsh, E.; Wuttrich, K. *Science* **1991**, *254*, 974.
(59) Gaigeot, M. P.; Sprik, M. *J. Phys. Chem. B* **2003**, *107*, 10344.
(60) Macleod, N. A.; Simons, J. P. *Phys. Chem. Chem. Phys.* **2004**, *6*, 2878.
(61) Alagona, G.; Ghio, C. *THEOCHEM* **2007**, *811*, 223.

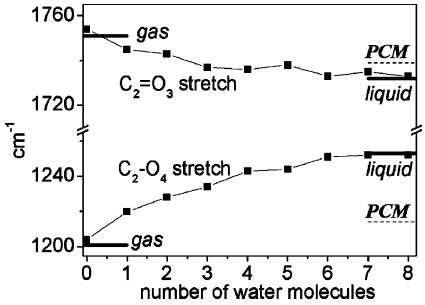

Figure 9. Variation of the C_2-O_4 and $C_2=O_3$ stretch frequency of $(\text{acetylcholine}-(\text{water})_{N=1-8})^+$ cluster ions as a function of *N*. Acetylcholine is in conformation III. The solid lines provide the experimental values in the gas phase (left) and acidified water (right). The dotted lines (right) provide predicted PCM values.

IR absorption spectra of $(\text{acetylcholine}-(\text{water})_{N=1-8})^+$ cluster ions have been calculated at the B3LYP/6-31G* level following optimization of cluster structures built by adding water molecules to the five gas-phase conformations of acetylcholine. Those cluster structures are not necessarily the lowest-energy structures but have been constructed by first solvating the C=O group and then progressively adding water molecules to the previously optimized cluster structures. Some stable structures of $(\text{acetylcholine}-(\text{water})_{N=8})^+$ cluster ions are presented in Figure 8. They correspond to acetylcholine$-(\text{water})_8$ cluster ions (conformation V) and PCM calculations (conformation III). The dipole moments of the water molecules tend to be electrostatically aligned by the positive charge of the quaternary ammonium. Water molecules are hydrogen-bonded either to the $C_2=O_3$ group or between themselves. Hydrogen bonding also takes place between water molecules and methyl groups. From simulations of the experimental broad-band IR spectrum, we can draw some qualitative conclusions. Water molecules do not likely directly bind to the ester oxygen O_4. Moreover, when a water molecule is forced to hydrogen bind to this atom, the calculated shift of the C_2-O_4 stretch with respect to the gas-phase value is twice as large as the observed shift. Hydrogen binding of a single water molecule to the carbonyl oxygen O_4 is not sufficient. On the contrary, binding of two water molecules to this atom provides a much too large shift. The best agreement between simulated and observed spectra is obtained when two water molecules are bound to O_4 in presence of several other water molecules. The role of those other water molecules is similar to the bulk water molecules that tend to slightly pull away the ones more strongly bound to the O_4 atom. The experimentally observed blue-shift of the C_2-O_4 stretch is not due to hydrogen bonding of the ester oxygen but to hydrogen bonding of the carbonyl oxygen.

We have plotted the frequencies of the two main spectral features, around 1200 cm^{-1} (C_2-O_4 stretch) and 1730 cm^{-1} ($C_2=O_3$ stretch), as a function of the number *N* of water molecules (Figure 9). In the case of acetylcholine conformer V and $N = 8$, we obtain a very satisfying agreement between simulation and experiment. For comparison, we have also calculated vibrational spectra with the less computationally expansive polarizable continuum model (PCM) that has been used in ref 18 for structural studies.

The respective blue (+52 cm^{-1}) and red (−19 cm^{-1}) shifts of those lines, which are experimentally observed in between the gas phase and liquid phase, are reproduced after addition of eight water molecules. As already stated, those eight

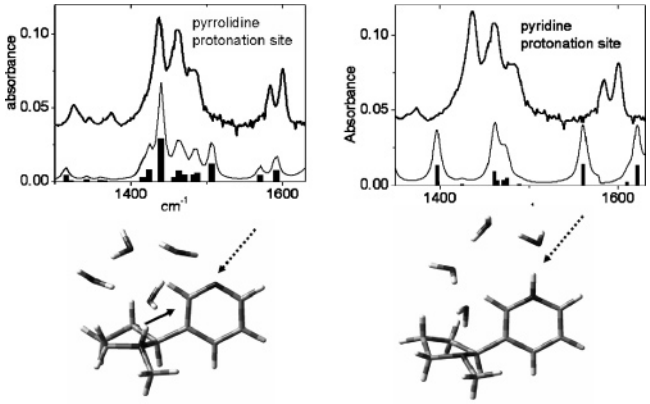

Figure 10. Experimental FT-IR spectrum of nicotine in an acidified water solution in the NH^+ bend spectral region. The left and right simulated spectra correspond respectively to nicotine protonated on the pyrrolidine (conformation II) and on the pyridine cycle (conformation I) in a $(\text{nicotine}-W_4)H^+$ cluster.

molecules do not constitute the full solvation shell of acetylcholine but rather the local solvation shell of the considered pharmacophoric groups. In contrast, the PCM model ($\epsilon = 78.38$) provides a blue-shift value of 13 cm^{-1} and a red-shifted value of 12 cm^{-1} far from the experimentally observed shifts.

Acetylcholine conformations mostly result from the competition between the $N_7C_6C_5O_4$ (θ_1) and $C_6C_5O_4C_2$ (θ_2) torsion strains on one side and the charge-induced dipole interaction between N_7^+ and $C_2=O_3$. In the PCM model, we can expect that the latter interaction is strongly decreased due to the change of a dielectric constant between the gas and the aqueous phase. In the cluster model, the water H-bonding network enters the competition. Indeed, we observe important structural modifications. Among the five conformations predicted and observed for bare acetylcholine, only four conformations subsist in the hydrated clusters after relaxation of geometries. Conformations II and IV are only very slightly modified by the presence of water. The torsion angle $\theta 1$ of conformation V is strongly modified (see Supporting Information). The cluster model allows us to follow the modification of the conformational space when water molecules are progressively added. With a single water molecule, conformation I still exists while it coalesces into conformation III in the presence of two water molecules.

4.2. Nicotine. In order to investigate the change of protonation site occurring in between the gas phase and the aqueous phase,[2] we have calculated $(\text{nicotine}-(\text{water})_{N=1-8})H^+$ structures and simulated infrared absorption spectra at the B3LYP/6-31G* level for each of the two lowest-energy conformations assuming either the pyrrolidine (N_{12}) or the pyridine (N_1) cycle as the protonation site. The energetically favored site is N_1 in the isolated molecule, and the presence of a single water molecule does not modify this situation. Adding a second water molecule allows the establishment of a bridge between the two cycles and strongly modifies the nicotine structure.[17] Following the addition of a third water molecule, we found a barrier-free proton-transfer path. If a proton is initially set on N_1 in a $(\text{nicotine}-(\text{water})_{N=3})H^+$ cluster, it first transfers onto the neighboring water molecule during the course of cluster optimization and ends on the N_{12} atom. However, even in the case of four added water molecules, we also found cluster structures with large barriers for proton transfer. This allowed us to simulate IR spectra of hydrated nicotine protonated on the pyridine cycle (Figure 10). In

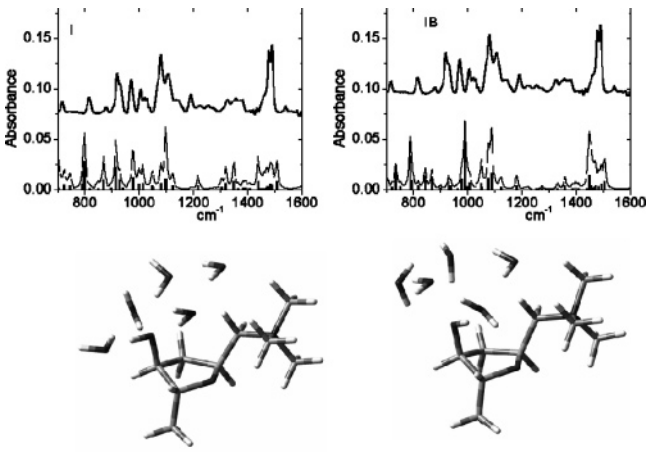

Figure 11. Experimental FT-IR spectrum of muscarine in an acidified water solution (top). The simulated spectra (bottom) correspond respectively to conformations I (left) and IB (right) of protonated muscarine microsolvated with five water molecules, as calculated at the B3LYP/6-31G* level.

(nicotine−(water)$_{N=8}$)H^+ clusters, we observed that proton transfer always takes place. The lowest-energy structure then becomes nicotine in conformation II protonated on the pyrrolidine cycle. Conformation I then lies 15 kJ/mol above conformation II.

The experimental broad band IR spectrum of nicotine in conformation II in an acidified aqueous solution is displayed in Figure 10. A satisfying simulation of the IR absorption spectrum of nicotine in an acidified water solution requires the presence of at least four water molecules in a nicotine−water cluster. The corresponding structure is not chosen as the lowest-energy conformation but corresponds to a water tetramer that solvates the $N_{12}-H^+$ group (Figure 10). The group of spectral lines around 1450 cm^{-1} of the experimental spectrum corresponds to in-plane and out-of-plane $N-H^+$ deformations. It is obviously missing in the calculated spectra when the proton is assumed to be on N_1 in the pyridinic cycle. On the contrary, this group is well reproduced when the proton is assumed in the pyrrolidine cycle. This observation is in agreement with the assumption that the biologically active protonation site of nicotine in aqueous solution is the pyrrolidine cycle.[6,62]

4.3. Muscarine. The infrared absorption spectrum of muscarine in an acidified water solution is presented in Figure 11. In contrast with acetylcholine and nicotine, this spectrum is rather similar to the gas-phase spectrum presented in Figure 6. In particular, the gas-phase spectral lines at 1085 and 1104 cm^{-1} are only shifted to 1081 and 1108 cm^{-1}. These lines correspond to the C_2-O_3 stretch and are slightly dependent upon the $O_{10}H_{32}$ group orientation. In muscarine−water clusters, this group of muscarine is bound to an accepting water molecule in which the dipole moment is submitted to the electrostatic interaction of the positively charged quaternary ammonium. Optimization of (muscarine−$W_{N=1-5}$)$^+$ cluster structures at the B3LYP/6-31G* level (Figure 11) shows that conformations I and IB of muscarine are still present but that conformation IA becomes absent. The torsion angle $C_2C_1O_{10}H_{32}$ of conformation I is not modified with respect to the gas-phase value while that of conformation IB decreases from 75° (Table 4). Conformation I remains the most stable, and the energy difference with conformation IB is lowered down to 4.15 kJ/mol. This energy differences with conformations IV, III, and II become respectively equal to 20.5, 21, and 44 kJ/mol. In a hydrated cluster, only conformations I and IB are thus populated at room temperature. IR spectra simulated from cluster structures I and IB are compared in Figure 11 with the experimental absorption spectrum of muscarine in acidified water. The fair agreement confirms the predicted existence of these two conformations.

Table 3. Distance d_{N7-O3} (d_{N7-O4}) between Nicotinic and Muscarinic (in Parentheses) Pharmacophores of Acetylcholine in the Gas Phase, in an ACh−W_8 Cluster, and with a PCM Model Calculated at the B3LYP/6-31G* Level for the Different Conformations

conformation	I	II	III	IV	V
gas phase	3.55	4.24	5.03	5.13	3.75
	(3.31)	(3.18)	(3.03)	(3.73)	(3.75)
ACh−W_8	-	4.71	4.87	5.2	4.61
cluster	-	(3.14)	(3.08)	(3.73)	(3.78)
PCM model	-	4.55	5.07	5.18	4.36
	-	(3.15)	(3.11)	(3.73)	(3.78)

5. Gas- and Aqueous-Phase Conformational Spaces and Relationship with Bioactivity

Since the proposed division into nicotinic and muscarinic pharmacological actions of acetylcholine in 1914,[63] establishment of relationships between structure and activity of ligands binding to acetylcholine receptors constitutes a very active field of research.[7,64−68] The development of therapeutic compounds takes advantage of a detailed knowledge of the exploration of conformational spaces of those ligands, such as, for example, epibatidine for its analgesic properties[7,69] or cytisine for fighting tobacco addiction.[70] From those studies, preferential distances between pharmacophoric groups in active conformations have been proposed and are in the range of 4.4−5.5 Å for nicotinic activity[69] and 3.2−3.8 Å for muscarinic activity,[63,71] involving respectively either a N^+-N or N^+-O distance. Distances are not the only crucial parameters since some dihedral angles seem to also play a role.[63]

The pharmacophoric groups, generally accepted as responsible for the nicotinic or muscarinic activity of acetylcholine, are the quaternary ammonium (N_7) and respectively the carbonyl O_3 or ester O_4 atoms. The calculated N_7O_3 and N_7O_4 distances between pharmacophores in the gas and aqueous phase are summarized in Table 3. For comparison, the predictions of a PCM model are also given.

In a simulation, we have replaced the quaternary ammonium group by a simple positive charge located at the same position as the N_7 atom in the different conformations. We have then

(62) Elmore, D. E.; Dougherty, D. A. *J. Org. Chem.* **2000**, *65*, 742.
(63) Bikadi, Z.; Simonyi, M. *Curr. Med. Chem.* **2003**, *10*, 1241.
(64) Behling, R. W.; Yamane, T.; Navon, G.; Jelinski, L. W. *Proc. Natl. Acad. Sci. U.S.A.* **1988**, *85*, 6721.
(65) Brejc, K.; van Dijk, W. J.; Klaassen, R. V.; Schuurmans, M.; van der Oost, J.; Smit, A. B.; Sixma, T. K. *Nature* **2001**, *411*, 269.
(66) Broad, L.; Zwart, R.; Pearson, K.; Lee, M.; Wallace, L.; Mc Phie, G.; Emkey, R.; Hollinshead, S.; Dell, C.; Baker, R. *J. Pharmacol. Exp. Ther.* **2006**, *318*, 1108.
(67) Purohit, Y.; Grosman, C. *J. Gen. Physiol.* **2006**, *127*, 719.
(68) Novella Romanelli, M.; Gratteri, P.; Guandalini, L.; Martini, E.; Bonaccini, C.; Gualtieri, F. *ChemMedChem* **2007**, *2*, 746.
(69) White, R.; Malpass, J. R.; Handa, S.; Baker, S. R.; Broad, L. M.; Folly, L.; Mogg, A. *Bioorg. Med. Chem. Lett.* **2006**, *16*, 5493.
(70) Etter, J. F.; Lukas, R. J.; Benowitz, N. L.; West, R.; Dresler, C. M. *Drug Alcohol Dependence* **2008**, *92*, 3.
(71) Kier, L. B. *Mol. Pharmacol.* **1967**, *3*, 487.

Table 4. Distance d_{N1-N12} between Pharmacophores of Nicotine in the Gas Phase and in a (Nicotine−W_8)H^+ Cluster Calculated at the B3LYP/6-31G* Level

protonation site	pyrrolidine		pyridine	
conformation	I	II	I	II
gas phase	4.65	4.35	4.11	4.75
nicotine−W_8 cluster	4.66	4.38	-	-

Table 5. Distance d_{N7-O3} and Torsion Angle $C_2C_1O_{10}H_{32}$ between Pharmacophores of Muscarine in the Gas Phase and in a (Muscarine−W_5)$^+$ Cluster Calculated at the B3LYP/6-31G* Level

	gas phase			(muscarine–W_5)$^+$ cluster	
conformation	I	IA	IB	I	IB
$C_2C_1O_{10}H_{32}$ angle (deg)	280	208	80	282	5.1
d N_7-O_3 (Å)	2.995	2.98	2.99	3.03	3.08

noticed that the calculated red-shifts of the carbonyl (C_2═O_3) stretch as a function of the N_7—O_3 distances are nearly identical to those observed in real acetylcholine. Those red-shifts are univocally determined by the electrostatic influence of the positive charge upon the C═O stretch. Thus, the experimental values of the red-shifts of the carbonyl stretch provide clues to the conformation of acetylcholine through the N_7—O_3 distance between its pharmacophoric groups.

In isolated acetylcholine, only conformations III and IV fall in the bioactive range (and marginally conformation II).[63] In contrast, the N_7—O_3 distance in the four calculated hydrated structures possesses values in between 4.6 and 5.2 Å. In agreement with the predictions of PCM calculations,[18] we observe that the conformational flexibility of acetylcholine is reduced by the presence of water.

The predicted distances N_1N_{12} between pharmacophores in isolated nicotine are given in Table 4 when protonation takes place on either the pyridine or the pyrrolidine site. In the latter case, those distances are not significantly modified by the presence of water in an optimized (nicotine−$(water)_{N=8}$)H^+ cluster. They are in close agreement with those obtained with a PCM calculation in ref 18. From calculations and interpretation of our experimental infrared spectra, we also conclude that only conformation II is energetically accessible and observed. The predicted distance N_1N_{12} is then only slightly lower than the N_7O_3 pharmacophoric distance of acetylcholine in a hydrated cluster. Another important pharmacophoric parameter is the dihedral angle $N_{12}C_{11}C_5C_6$ (τ_1 in ref 63). Our cluster calculation provides a value of 105.8° in conformation II, close to the result of ref 18 obtained with a PCM model.

Muscarinic activity of acetylcholine is attributed to the existence of the N_7 and O_4 pharmacophoric atoms. In muscarine, the corresponding atoms are N_7 and O_3. As shown in Table 5, the distance d_{N7-O3} is only slightly affected by the presence of water. This can be understood from our calculation of the structure of the muscarine−water clusters. As in the acetylcholine hydration shell, the ester oxygen O_4 does not participate in the hydrogen bonds. On the contrary, water molecules solvate the $O_{10}H_{32}$ group and induce significant modifications of the $C_2C_1O_{10}H_{32}$ angle as shown in Table 5.

5. Conclusion

In the present work, we have experimentally recorded the infrared spectra of acetylcholine, nicotine, and muscarine in both the gas phase and aqueous solution. The relevance of gas-phase studies of molecules of biological interest can be questioned, and it is often quoted that relevant studies should be conducted in solution. In some cases, the situation can be intermediate. For example, in the modeling of cholinergic neurotransmission, only a very restricted number of water molecules are considered in the allosteric binding site of ligands to the nicotinic acetylcholine receptors.[72,73] For the interpretation of our aqueous-phase experimental data, we have chosen the use of an explicit water molecule model. As far as structural results are concerned, our results agree with those obtained by using a PCM model into which water is a continuous medium. On the contrary, the quantitative interpretation of our IR spectra requires the use of hydrated cluster calculations. The size of the clusters remains rather small since we are only concerned by modifications of vibrational frequencies induced by the presence of water molecules hydrogen-bonded to the concerned chromophores. If we admit that our cluster calculations are validated by our experimental data conducted in bulk water, we can follow the structural modifications induced by adding one-by-one water molecules in our simulations. In the case of acetylcholine, we find that the presence of only two water molecules is sufficient to reduce the number of accessible conformations. For isolated nicotine, we provide clear experimental evidence of protonation on the pyridine cycle. We show that the presence of at least three water molecules opens energetically favorable proton-transfer paths. This combination of gas-phase and condensed-phase experiments allows studying the changes in structure and pharmacophoric activity induced by the presence of explicit water molecules.

Acknowledgment. The authors thank the CLIO team for their technical help and Prof. Yves Bouteiller (Univ. Paris 13) for helpful discussions. The financial support of the European Commission is gratefully acknowledged (EPITOPES, Project No. 15637).

Supporting Information Available: Conformations of acetylcholine and acetylcholine ions; optimized coordinates of five structures of acetylcholine ions at the B3PW 91/6311++G-(d,p) level; time evolution plots of acetylcholine ions acetylcholine; assignment of experimentally observed spectral lines of gas-phase acetylcholine ions and muscarine ions; relative energies and free energies of different acetylcholine ion conformations, gas-phase nicotine ions, and muscarine ions; structure and coordinates of optimized acetylcholine−$(water)^+_8$ ions; and structure of first solvation shell calculated in a cage of 146 water molecules. This material is available free of charge via the Internet at http://pubs.acs.org.

JA710040P

(72) Iorga, B.; Herlem, D.; Barré, E.; Guillou, C. *J. Mol. Model* **2006**, *12*, 366.
(73) Amiri, S.; Sansom, M. S. P.; Biggin, P. C. *Protein Eng., Des. Sel.* **2007**, *20*, 353.